Journal of Radioanalytical and Nuclear Chemistry (2020) 323:365–377
https://doi.org/10.1007/s10967-019-06928-5

Study of adsorption performance and adsorption mechanism for U(VI) ion on modified polyacrylonitrile fibers

Fan Wang[1] · Xinglei Wang[1] · Yunjie Jiang[1] · Zhiwei Niu[1] · Wangsuo Wu[1,2,3] · Hongxia Zhang[1,2,3]

Received: 21 August 2019 / Published online: 5 November 2019

Abstract

The modified polyacrylonitrile fibers (ACPAN fibers) was synthesized by oximation reaction and alkaline hydrolysis. ACPAN fibers was characterized by means of SEM, FTIR, XPS and elementary analysis. The effects of contact time, solid–liquid ratio, pH, ionic strength, initial concentration and temperature on U(VI) adsorption onto ACPAN fibers was studied and the adsorption mechanism was also discussed. The experimental data fitted well pseudo-second-order kinetics model and Freundlich and D–R models, and thermodynamic process was an endothermic and spontaneous reaction. The maximum adsorption capacity was 163 mg/g, and U(VI) and ACPAN fibers possible formed more stable penta-coordination complexation. This paper highlighted ACPAN fibers as a good adsorbent to remove efficiently and economically uranyl from radioactive wastewater.

Keywords ACPAN fibers · Adsorption · Uranium

Introduction

Uranium is an important radioactive element, which has been widely used in the nuclear industry [1]. Uranium subsists in the environment due to leaching from mine tailings, natural deposits, use of uranium-containing phosphate fertilizers, emissions from the nuclear industry [2]. Furthermore, the chemical toxicity and radiotoxicity of uranium has tremendously aggravated health concerns with the increase of human activities with uranium [3]. In order to protect people's health and ecosystem environment, the effectively removal of U(VI) ions from the waste aqueous solutions has become crucial issues. Therefore, efficient technology for the removal or recovery of uranium from waste solution has become strongly demanded.

It is well known, the adsorption has been considered to be a remarkably efficient approach in these methods. At the moment, the types of adsorbents have been widely researched, such as inorganic materials and organic materials, including natural and synthetic materials [4–6]. By comparing, synthetic functionalized materials, which has high adsorption capacity and good selectivity for U(VI), have caused considerable concern. German researchers have found that the material with amidoxime (AO) functional group for recovery uranium was the most potential adsorbent [7, 8]. Japan researcher also has found the AO group is covalently bonded on PE-based fibers, which have a high adsorption capacity for uranium and have good mechanical strength [9]. Recently, there has been a new development about AO-based adsorbents that amidoximation of polyacrylonitrile (PAN) fibers reacts with hydroxylamine. The results show the fibers are an excellent adsorbent for uranium extraction [10]. Therefore, adsorbents contain the amidoxime group at least, which are the most potential adsorbents for uranyl recovery.

Polyacrylonitrile fibers, which have cheaper price and excellent tensile strength, have been widely used. But PAN fibers are hydrophobic, and could not adsorb metal

Electronic supplementary material The online version of this article (https://doi.org/10.1007/s10967-019-06928-5) contains supplementary material, which is available to authorized users.

✉ Hongxia Zhang
hxzhang@lzu.edu.cn

[1] School of Nuclear Science and Technology, Lanzhou University, Lanzhou 730000, China

[2] Key Laboratory of Special Function Materials and Structure Design, Ministry of Education, Lanzhou University, Lanzhou 730000, China

[3] Engineering Research Center for Neutron Application Technology, Ministry of Education, Lanzhou University, Lanzhou 730000, China

ions effectively, which limit further applications in waste solution [11]. After the alkaline treatments, the cyano functional groups of the PAN fibers could be converted to the carboxylates, meanwhile the fibers have good water retention behavior, and make them superabsorbent materials [12]. But few studies have been done about modified polyacrylonitrile fibers (ACPAN fibers) for sorption metals, especially the adsorption mechanism for metal ions is not very clear.

Based on previous studies, this work is to synthesize ACPAN fibers with high selectivity for uranium and hydrophilicity by modifying polyacrylonitrile fibers. The various influence factors were studied in detail. Besides, desorption experiments and the reusability of adsorbent was investigated as well. As far as we know, this is the first time to speculated the mechanism between UO_2^{2+} ion and ACPAN fibers by FTIR and XPS spectrum. The material was expected to be used for the recovery of uranyl from aqueous solution.

Experimental

Materials

All chemical reagents used are analytical grade. PAN fibers purchased were degreased by acetone, and then were dried at 40 °C. $UO_2(NO_3)_2$ solution was prepared by dissolving U_3O_8 in HNO_3 solution, then diluted with deionized water.

Preparation of ACPAN fibers

According to the preliminary experiment, ACPAN fibers of synthesis reaction can be divided into two major steps. (1) Synthesis of AOPAN fibers: PAN fibers was soaked in methanol, and sodium carbonate and hydroxylamine hydrochloride was dissolved in deionized water at pH 7, then the above two solution was placed in three flasks and refluxed for 3 h at 70 °C under the protection of N_2. Finally, the resultant was washed with deionized water and methanol alternately repeatedly, and dried in a vacuum oven for 24 h at 40 °C [10]. (2) Synthesis of ACPAN fibers: according to the preliminary experiment (Fig. SI1), AOPAN fibers was hydrolyzed in 0.2 M sodium hydroxide at 75 ± 1 °C, then the resultant was washed with deionized water and dried in a vacuum oven at 40 °C for 24 h. The resultant was ACPAN fibers.

Characterization of ACPAN fibers

The ACPAN fibers was characterized by scanning electron microscopy (SEM), elemental analysis, Fourier transform infrared spectroscopy(FTIR), and X-ray photoelectron spectroscopy (XPS). The hydrophilicity of fibers was characterized by water absorption. Namely, the fibers was immersed in deionized water at 25 °C for 24 h, then the fibers was taken out, finally the surface water of fibers was absorbed by filter paper and weighed again.

$$\text{Water absorption} = (m_0 - m_1)/m_0 \times 100\% \quad (1)$$

where m_0 and m_1 (g) are the quality of fibers before and after water absorption respectively [13].

Sorption experiment

The sorption experiments of U(VI) onto fibers were carried out by a batch technique. Namely, the fibers, $NaNO_3$ solution, and U(VI) solution was added in the polyethylene tubes. The pH of the solution was adjusted with negligible volume of HNO_3 or NaOH solution. The mixture was shaken in water bath, and then solid and liquid phases was separated by centrifugation. The concentration of U(VI) in the supernatant was analyzed by using a spectrophotometer at 650 nm with Arsenazo III. The adsorption percentage (%) and adsorption capacity (q_e) of U(VI) was calculated by the following equations:

$$\text{Sorption}\% = (C_\text{i} - C_\text{f})/C_\text{i} \times 100\% \quad (2)$$

$$q_\text{e} = (C_\text{i} - C_\text{f}) \times V/m \quad (3)$$

where C_i and C_f (mmol/L) is the initial and final concentration of U(VI) in the solution, respectively. m is the mass (g) of fibers, and V (L) is the volume of the solution.

Desorption experiment

The uranyl-loaded ACPAN fibers was washed with distilled water, and transferred into the solution and shocked for 24 h, then centrifuged. The amount of U(VI) released into the solution was monitored by the previous method in the adsorption experiment. The U(VI) recovery percent (%) was calculated using the following equation:

$$\text{Recovered}\% = n_\text{de}/n_\text{ad} \times 100\% \quad (4)$$

where n_ad and n_de (mmol) was initially adsorbed and desorbed U(VI) amount on the ACPAN fibers, respectively. The adsorption/desorption cycles were repeated five times using the same batch method.

Results and discussion

Characterization of fibers

Figure SI2a, b showed SEM images of PAN fibers and ACPAN fibers in different magnification. The surface of PAN fiber was rather smooth and compact. After oximation reaction and hydrolysis under alkaline conditions, the surface of ACPAN fibers became looser and rougher [14].

For PAN fibers, AOPAN fibers, and ACPAN fibers, elemental percentage of N, C and H by elemental analysis method was shown in Table 1. The C/N value of AOPAC fibers was lower than that of PAN fibers, which proved that the part of cyano groups on PAN fibers was converted into amidoxime group, while the C/N value of ACPAN was higher than that of AOPAN fibers, indicating that the part of oxime groups of AOPAN fibers was hydrolyzed to carboxyl groups of the ACPAN fibers. The conclusion was explained by FTIR (Fig. 1). Fig. SI3 showed the full survey XPS scan of the ACPAN fibers, and Fig. SI4 showed EDS spectrum of the ACPAN fibers, which demonstrated ACPAN fibers were mainly composed of C, N and O. Water adsorption on PAN fibers and AOPAN fibers was 37%, 53%, while water adsorption on ACPAN fibers was 97% and showed in Fig. SI5. The result illustrated the ACPAN fibers is a good hydrophobic material.

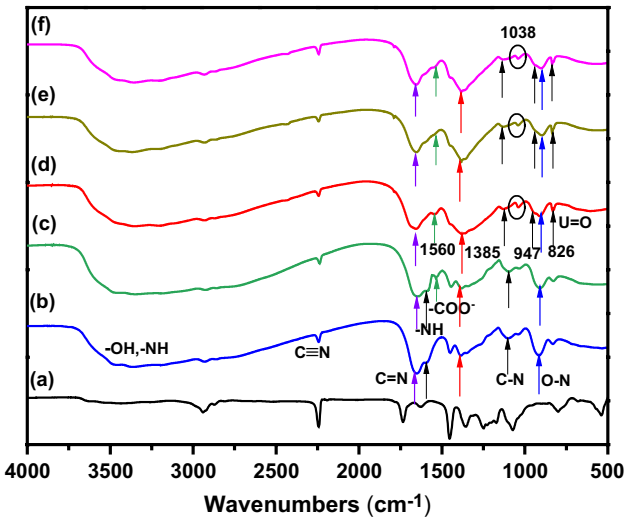

Fig. 1 FTIR spectra of PAN fibers (a); AOPAN fibers (b); ACPAN fibers (c); and uranyl-loaded ACPAN fibers at pH 3, 5, 8 (d–f)

The FTIR spectra of PAN fibers, AOPAN fibers and ACPAN fibers were shown in Fig. 1. Figure 1a exhibited the absorption peaks of a stretching vibration at 2241 cm^{-1} (C≡N), which suggested that the PAN was a copolymer of acrylonitrile [14]. In Fig. 1b, compared with Fig. 1a, C≡N stretching vibrations peaks weaken in intensity and new bands at 1652 cm^{-1} and 912 cm^{-1} corresponding to stretching vibration of C=N and N–O appeared, indicating the conversion of C≡N to C=N [12], and additional peak at 1590 cm^{-1} was due to the bending vibration of –NH in amidoxime fibers [15]. The broad absorption peaks at 3000–3700 cm^{-1} was observed –OH overlapped with –NH stretching bands, and can be attributed to H-bonding of NH and –OH in the amidoxime structure. After the hydrolysis reaction under alkaline condition (in Fig. 1c), appearance of the new peak at 1550 cm^{-1} ascribed to carboxylate group [16], which probably came from the hydrolysis of the partial amidoxime group under NaOH conditioning [17].

Effect of contact time

Contact time is a very important factor for adsorption, which depends on the metal ions and adsorbent. Figure 2a showed the effect of the contact time on U(VI) adsorption on ACPAN fibers. At first, the speed of U(VI) adsorption

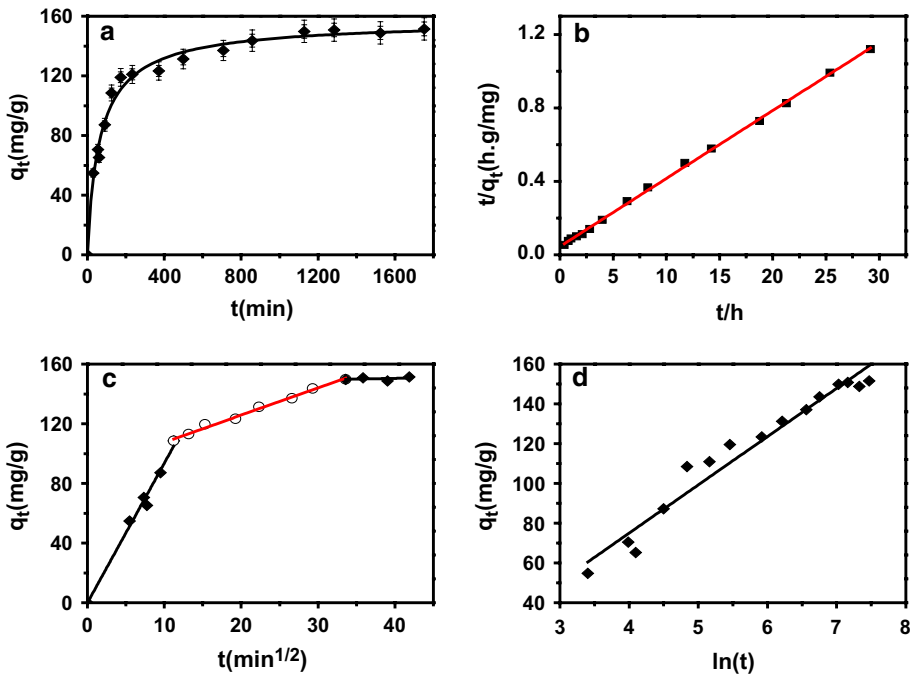

Fig. 2 Effect of contact time on the adsorption of U(VI) onto ACPAN fibers (**a**); pseudo-second order rate model (**b**); intra-particle diffusion model (**c**); Elovich model (**d**), error bars represent standard deviation about the average, $C_0 = 4\times10^{-4}$ mol/L, pH = 5.0 ± 0.1, $m/V = 1$ g/L, $T = 298 \pm 1$ K

Table 1 The elements of composite for PAN fibers, AOPAN fibers and ACPAN fibers

Samples	Nitrogen%	Carbon%	Hydrogen%	Oxygen%	C/N
PAN fibers	23.02	68.34	5.93	2.71	2.97
AOPAN fibers	20.11	44.46	7.16	28.27	2.21
ACPAN fibers	16.41	41.69	5.98	35.92	2.54

on the ACPAN fibers was very rapid, then slowed down with increasing contact time. This was attributed to the fact that vacant adsorption sites of ACPAN fibers were sufficient at the beginning. With the adsorption proceeding, the nonbonding functional groups existing on the ACPAN fibers decreased, which could not easily be occupied due to the repulsive forces between the UO_2^{2+} and ACPAN fibers. Therefore, the interactions with the UO_2^{2+} and ACPAN fibers became more difficult.

In order to clearly describe the kinetic mechanism of U(VI) on ACPAN fibers, pseudo-first-order model, pseudo-second-order model, intra-particle diffusion model, and Elovich model were used to fit the experimental data. The details of the models were attached in SI2. The fitting parameters of the four models were listed in Table 2. It can be seen that pseudo-second-order model fit better than pseudo-first order rate model (related Fig. 2 was not involved) with higher correlative coefficients (R^2), which explained that adsorption of U(VI) ions on ACPAN fibers followed well pseudo-second-order kinetics. The result also suggested that adsorption process belonged to chemical adsorption, and chemical adsorption played a dominant role, which involved binding forces through chelation or electron transfer between uranyl, carboxyl and amidoxime group on ACPAN fibers [18]. Figure 2c showed the adsorption of U(VI) on ACPAN fibers of intra-particle diffusion model. According to SI Eq. (3), the plot of q_t versus $t^{1/2}$ should be a straight line through origin of coordinates [19]. However, the plot of Fig. 2c showed that adsorption pattern did not go through the origin, but it occurred in three stages. The first stage was fast kinetics of the external surface or instantaneous adsorption,

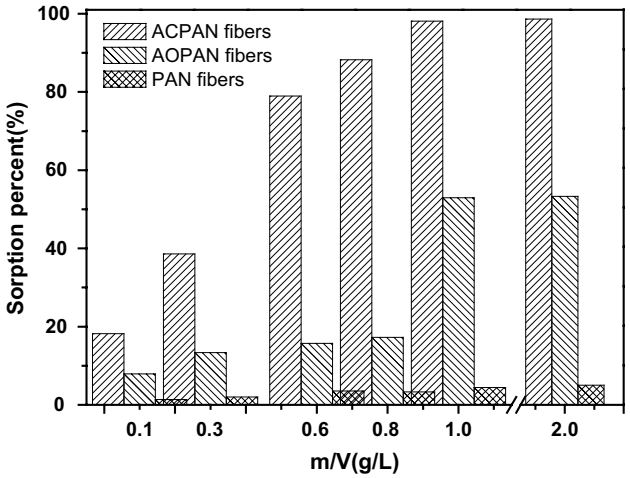

Fig. 3 Effect of solid content on the adsorption of U(VI) on three fibers, $I=0.1$ mol/L, pH = 5.0 ± 0.1, $C_0=4\times10^{-4}$ mol/L, $T=298\pm1$ K, $t=48$ h

and the second stage was the gradual adsorption stage, therefore intraparticle diffusion was rate-controlled, and the third stage was the final adsorption equilibrium [20]. Meanwhile, the slope of line in the second stage was called intraparticle diffusion rate constant(k_{int}) [21], which displayed in Table 2. From Table 2, R^2 illustrated that the intraparticle diffusion model followed well the experimental data. Therefore, the mechanism of U(VI) adsorption on the ACPAN fibers was complex, and intraparticle diffusion contributes to the actual adsorption process. Similar adsorption process has already been reported [21].

Effect of solid–liquid ratio

The effect of solid–liquid ratio of kinds of fibers and the solution on the adsorption of U(VI) ions was carried out from 0.1 to 2.0 g/L in Fig. 3. The removal efficiency of the U(VI) ions increased with increasing the amount of adsorbent, and attained the maximum adsorption at 1.0 g/L of solid–liquid. Figure 3 also showed the adsorption capacity

Table 2 Kinetic parameters for uranyl obtained from models on the ACPAN fibers

Pseudo first-order kinetic equation		Pseudo second-order kinetic equation	
q_e (mg/g)	150.08	q_e (mg/g)	163.98
K_1 (h^{-1})	1.0244	K_2 (g h/mg)	0.0052
R^2	0.6615	R^2	0.9992
The intraparticle diffusion model		The Elovich equation	
K_{int} (mg/g $min^{1/2}$)	1.8209	α (mg min/g)	9.7593
C	89.3699	β (g/mg)	0.0412
R^2	0.9909	R^2	0.9556

on the ACPAN fibers was the largest, while the adsorption capacity on PAN fibers was the smallest. The removal efficiency (%) of U(VI) ions increased from 1.3% to 8.9%, 7.8% to 52% and 18% to 99% with increasing the dosage of PAN fibers, AOPAN fibers and ACPAN fibers from 0.1 to 2.0 g/L, respectively. Therefore, the increase of U(VI) adsorption percent on the fibers with solid–liquid ratio increasing was attributed to the increase surface of active site on the fibers. Meanwhile, the total available adsorption sites of the PAN fibers, AOPAN fibers and ACPAN fibers were increased for the metal chelate and/or ion-exchange.

Effect of pH

The effect of pH on the U(VI) adsorption onto fibers was investigated in pH 2–9, and the results were shown in Fig. 4a. As can be seen from the Fig. 4a, the adsorption percent of U(VI) on three kinds of fibers increased and then decreased with pH increasing.

To further properly explain the U(VI) adsorption behavior, the surface charge of the fibers and the species of uranium is important at different pH. The surface charge of fibers can be known by measuring the zeta potential of fibers, and was shown Fig. 4b. Uranyl species in the absence of adsorbent at different pH was calculated using Visual MINTEQ 3.1 software and presented in Fig. 4c. The prominent U(VI) species are UO_2^{2+}, UO_2OH^+, $(UO_2)_2(OH)_5^+$, $(UO_2)_4(OH)_7^+$ at pH 2.0–6.5. As shown in Fig. 4b, the surface of the fibers is positively charged prior to zero potential, while the surface of the fibers is negatively charged after zero potential. The adsorption of U(VI) on fibers was different due to the electrostatic repulsion and or attraction (positively charged species and protonation or deprotonation of fibers). The strong interaction between the positively charged species and deprotonation enhanced the adsorption of U(VI) with increasing pH; then the decrease of U(VI) adsorption on fibers with pH increasing can be attributed to repulsion of negative charge U(VI) species [i.e., $(UO_2)_2CO_3(OH)_3^-$, $UO_2(CO_3)_2^{2-}$, $UO_2(CO_3)_3^{4-}$ in Fig. 4c] and deprotonation. To be specific, at lower pH, ACPAN fibers of carboxyl and amphiprotic AO groups was protonated and bacome positively charged, and UO_2^{2+} dominated at lower pH (in Fig. 4c), therefore the repulsive force between protonated AO, COOH and UO_2^{2+} acted as an unfavorable factor for the coordination. At this moment, H^+ in the solution would compete with the UO_2^{2+} ions for the adsorption sites on the surface of the adsorbent. Hence, the adsorption amount of uranyl was lower. With pH increasing, AO and COOH groups became to deprotonated to generate $-COO^-$ and AO^- and the electrostatic attraction between UO_2^{2+} and AO^- (or COO^-) favored the binding of uranyl and the adsorbent. As pH continued to increase (pH > 5.2), (see Fig. 4c), UO_2^{2+} ions began to hydrolyze. Especially,

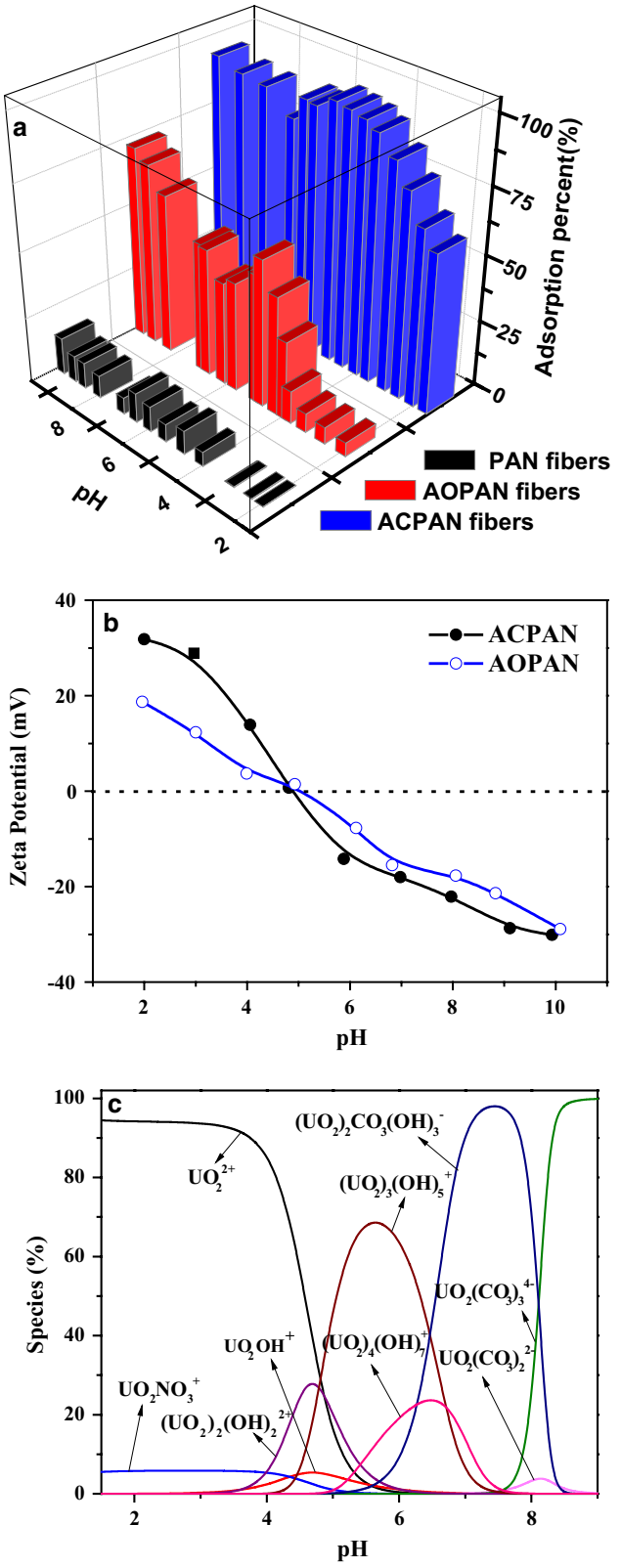

Fig. 4 Effect of pH on the adsorption of U(VI) on three fibers (**a**), $I=0.1$ mol/L, $C_0=4\times10^{-4}$ mol/L, $T=298\pm1$ K, $t=48$ h; Zeta potential of ACPAN fibers (**b**); distributions of U(VI) species in 4×10^{-4} mol/L, $I=0.1$ mol/L solutions with atmospheric CO_2 are plotted versus pH by the Visual MINTEQ 3.1 software simulation of the uranium (**c**)

CO_3^{2-} can form strong carbonate uranyl complex in the presence of CO_2 in the air. Therefore, pH > 7, the main species of $UO_2(CO_3)_2^{2-}$ and $UO_2(CO_3)_3^{4-}$ led to weaker adsorption between U(VI) and ACPAN fibers. Until pH increased to 9, the adsorption capacity increased again, probably because of the precipitation of uranyl under alkaline conditions [22], which was verified through blank uranyl precipitation experiment at the same condition without fibers added.

By comparison, ACPAN fibers was much more effective to remove U(VI) than the other fibers. The maximum percentage of U(VI) removed was 8.9%, 52%, 99% on three fibers, respectively(in Fig. 4a). On one hand, because carboxyl is a hydrophilic group, which made ACPAN fibers be more hydrophilic than PAN and AOPAN fibers and the results showed in Fig. SI5; On the other hand, the surface of PAN fibers had little active sites adsorbed, and AOPAN fibers had the ability to chelate with UO_2^{2+} by using the lone pair electrons of oxime group O atom and amino N atom [23], while ACPAN fibers had carboxyl and amidoximate groups, and carboxyl groups on ACPAN fibers was conducive to dissociate uranyl hydrolyzed and uranyl carbonate ion [8], which promoted U(VI) and ACPAN fibers formed more stable complexes.

Effect of the initial concentration

The initial concentration of U(VI) directly affects the capacity and efficiency of the adsorbent. The relationship between adsorption amount (or adsorption percent) and the initial U(VI) concentration was displayed in Fig. 5. The adsorption amount increased rapidly with the increase of the initial concentration of U(VI) within the range of 0–4×10^{-4} mol/L, because the higher concentration of U(VI) accelerated the diffusion of U(VI) ions from solution to the adsorbent surface [24]. In addition, when more U(VI) ions was present in the solution, a higher fraction of available active sites took part in the adsorption process [25]. This could be attributed to the hydration of the exposed hydrophilic groups on the fiber surface. Meanwhile, the adsorption approached the saturation plateau with initial uranyl concentration increasing from 4×10^{-4} mol/L to 8×10^{-4} mol/L, because the surface active sites were fully covered or the extent of adsorption reached the limit in saturated adsorption. Therefore, further increase of U(VI) ion concentrations did not change the equilibrium adsorbed amount. Similar phenomenon was also observed in the uranium sorption by synthesis of amidoximated polyacrylonitrile fibers and amidoximated poly(AN/N-vinylimidazole) copolymeric hydrogels [25, 26].

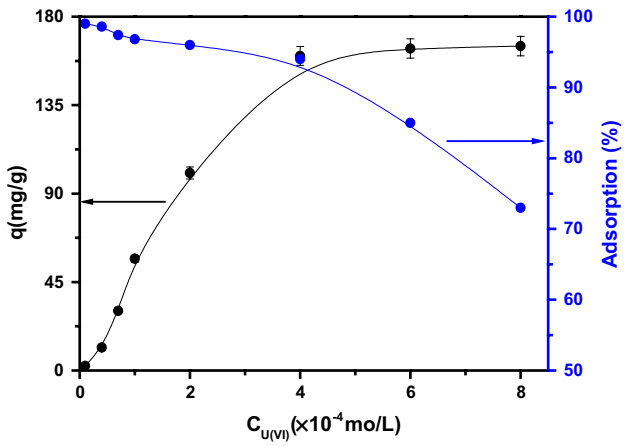

Fig. 5 Effect of the initial concentration of U(VI) on adsorption capacity and adsorption (%) onto ACPAN fibers, error bars represent standard deviation about the average. $I = 0.1$ mol/L, pH = 5.0 ± 0.1, $T = 298 \pm 1$ K, $t = 48$ h

Effect of ionic strength

Ionic strength is an important factor for adsorption. In most adsorption systems, the increase of ionic strength will decrease the adsorption capacity, because cations of electrolyte (Na^+) will compete with radionuclides for the sorption sites on the sorbent surface [27]. On the contrary, cations of electrolyte (Na^+) could increase the zeta potential value of adsorbents, resulting in increasing the electrostatic attraction. Therefore, the adsorption will increase with the increase of ionic strength [28, 29]. However, the adsorption of U(VI) on the ACPAN fibers had no significant influence on with $NaNO_3$ concentration increasing under the experimental conditions (0–1.0 mol/L), which was shown in Fig. 6. It may be the addition of Na^+ suppressed the electrostatic attraction between the positively-charged U(VI) species and deprotonated carboxyl or amidoxime groups of the ACPAN fibers by electrostatic screening effect [30]. This result has also reported in previous literature [31]. Therefore, it was deduced that the effect of $NaNO_3$ on U(VI) adsorption was the synergistic effect of the promotive salting-out effect and the inhibitive electrostatic screening effect [30]. From this point of view, the electrostatic forces should be considered only a minor reason for U(VI) adsorption on ACPAN fibers. The similar result was also reported [32]. Since ionic strength had no obvious impact on the adsorption capacity of UO_2^{2+} on the ACPAN fibers, suggesting that the sorption mechanism of U(VI) and ACPAN fibers was inner-sphere surface complexation under experimental conditions [32]. Therefore, the ACPAN fibers is a promising material of adsorption especially from high saline aqueous media. This also indicated that ACPAN fibers could be more suitable for recovery of U(VI) ions from sea water.

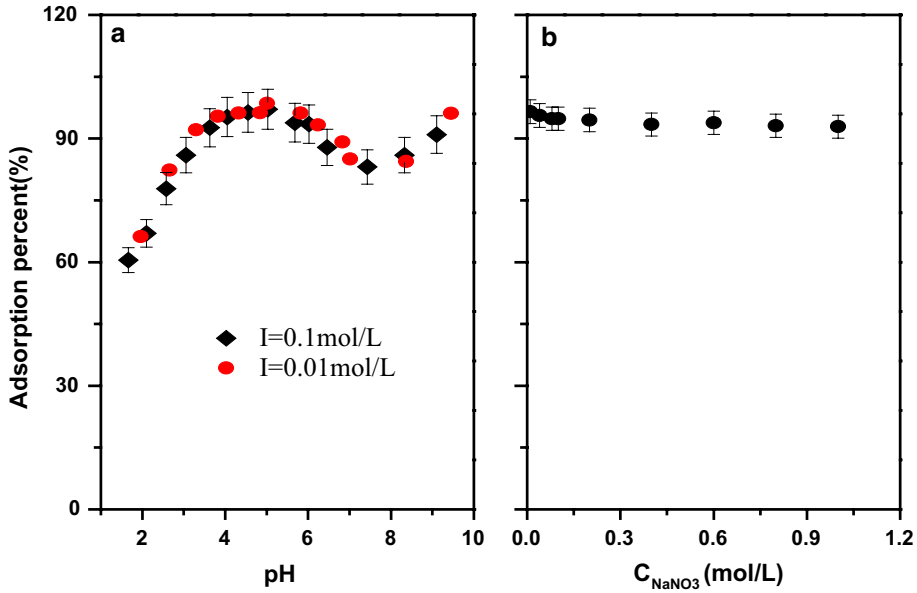

Fig. 6 The adsorption of U(VI) on ACPAN fibers at different ionic strength, $m/V=1$ g/L, $C_0=4\times10^{-4}$ mol/L, $T=298\pm1$ K, $t=48$ h. Error bars represent standard deviation about the average

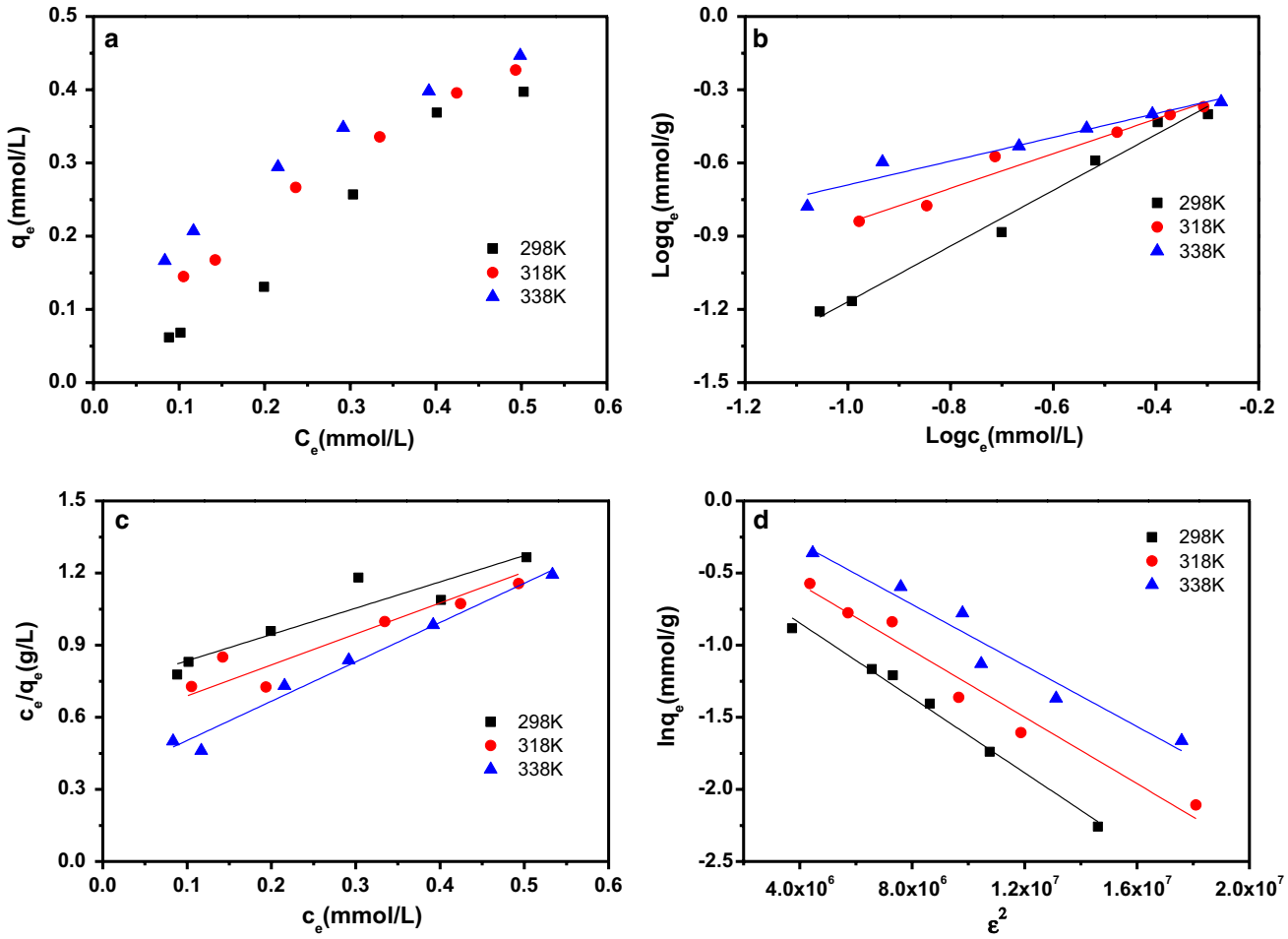

Fig. 7 Effect of the solution temperature on U(VI) adsorption onto ACPAN fibers (**a**); $I=0.1$ mol/L, pH $=5.0\pm0.1$, $m/V=1$ g/L, $t=48$ h Freundlich model (**b**); Langmuir model (**c**) and D–R model (**d**)

Effect of the temperature

It is necessary to study the adsorption of the radionuclides on the material at different temperatures. The adsorption experiment of U(VI) on ACPAN fibers at 25, 45, and 65 °C was carried out and the results were shown in Fig. 7a. The adsorption capacity of uranyl on ACPAN fibers increased with raising the temperature. A possible explanation is that elevated temperature increases the activity of functional groups of adsorbent, and promotes the diffusion of uranyl ions. [33].

In order to further explain the nature of the adsorption process and the adsorption mechanism, The data of adsorption for U(VI) ions on ACPAN fibers was simulated by three adsorption models: Freundlich, Langmuir, and Dubinin–Radushkevich. The equations of the adsorption models were represented in SI2 in detail. Meanwhile, Langmuir, Freundlich and D–R parameters of adsorption with their standard errors were completed by a commercial software program (SPSS10.0). Mean weighted square errors (MWSE) are calculated by Eq. (5):

$$\mathrm{MWSE} = \frac{(q_{\mathrm{exp}} - q_{\mathrm{cal}})^2}{nq_{\mathrm{exp}}^2} \tag{5}$$

where q_{exp} and q_{cal} (mmol/g) is the experimental data and the calculated value according to corresponding isotherm model, respectively. n refers to the degrees of freedom ($n = N - 2$), N is the number of experimental point [34].

The Freundlich isotherm constants K_{F} and n were determined (shown in Table 3). K_{F} increased with elevating temperature, which indicated that the adsorption process was endothermic. $n > 1$ reflected a high affinity between ACPAN fibers and U(VI) ions [8]. The Freundlich isotherm well fitted experimental data as referred from R^2 in Table 4. q_{max} value obtained from Freundlich model was close to that experimentally obtained. For Langmuir model, q_{m} and K_{α} calculated by Fig. 7c and showed in Table 3. Langmuir isotherm model cannot well fit the experimental data of U(VI) adsorption on ACPAN fibers from R^2 values(in Table 3).

For D–R model, q_{m} values were consistent with q_{m} values previously determined from Freundich model. The correlation coefficients (R^2) of D–R model was better as compared to Langmuir isotherm model (Fig. 7d, Table 3). E value is very useful for estimating the type of sorption reaction in D–R model. If $E < 8$ kJ/mol, the sorption may be affected by physical forces; when E is 8–16 kJ/mol, chemical ion-exchange governs the adsorption process; while $E > 16$ kJ/mol, the adsorption may be dominated by particle diffusion [35]. E values obtained by SI [Eq. (9)] were 21.74, 21.33 and 20.82 kJ/mol. Therefore, the adsorption process of U(VI) onto ACPAN fibers is controlled adsorption processes by diffusion as reported by Glasstone et al. [36]. The result is consistent with the previous research of intraparticle diffusion model.

Table 4 Thermodynamic parameters of U(VI) adsorption on ACPAN fibers

T (K)	ΔG (kJ/mol)	ΔS [J/(K mol)]	ΔH (kJ/mol)
298.15	− 21.84		
318.15	− 24.41	128.01	16.32
338.15	− 26.97		

Table 3 Adsorption parameters of Langmuir, Freundlich and D–R model for U(VI) on ACPAN fibers

Model	T (K)	298	318	338
Langmuir	K_{L} (L/mol)	0.4392	0.4541	0.4398
	q_{max} (mmol/g)	0.6114	0.6740	0.7174
	MWSE	0.0634	0.0592	0.0249
	N	6	6	6
	R^2	0.8456	0.8734	0.9756
Freundlich	n	1.1423	1.4092	2.0531
	K_{F} (mol^{1-n} L^n/g)	9.3274	8.0114	8.0421
	q_{max} (mmol/g)	0.6301	0.6301	0.6301
	MWSE	0.0223	0.0235	0.0241
	N	6	6	6
	R^2	0.9848	0.9577	0.9331
D–R	β (mol^2/kJ^2)	1.057×10^{-7}	1.098×10^{-7}	1.153×10^{-7}
	q_{max} (mmol/g)	0.5109	0.6246	0.71
	MWSE	0.0228	0.0226	0.0302
	N	6	6	6
	E (kJ/mol)	21.74	21.33	20.82
	R^2	0.9853	0.9864	0.9585

In order to further understanding of the adsorption process, the thermodynamic data(ΔG^0, ΔH^0 and ΔS^0) calculated by SI (Eqs. (10–11)) and Fig. SI6 were reported in Table 4. The negative value of ΔG^0 confirmed the spontaneity of the adsorption process. The value of ΔG^0 became more negative with the increase of temperature, which explained more efficient adsorption at higher temperature [37]. This was because U(VI) ions were readily dehydrated at higher temperatures, which led to adsorption to be more favorable [27]. Meanwhile, the positive value of ΔH^0 suggested that adsorption of U(VI) ions on ACPAN fibers was endothermic reaction. This was because the desolvation process requires more energy than that released in the adsorption process [38, 39]. In addition, it was a strong bond between the adsorbate and adsorbent from the magnitude of ΔH^0, as reported by Gupta [16]. The result was consistent with the previous result analyzed by Frendlich model. The values of ΔS^0 were far greater than zero, which showed the entropy to increase during the adsorption process. Meanwhile, positive values of ΔS^0 suggested there was the strong sorption between U(VI) sorption and ACPAN fibers by inner-sphere surface complexation [29]. The result was consistent with the previous results on the influence of ionic strength.

Adsorption selectivity of ACPAN fibers

The adsorption of other metal ions on ACPAN fibers was also studied and the results were shown in Fig. 8. The ACPAN fibers exhibited higher adsorption efficiency and good adsorption selectivity for U(VI) rather than other elements by distribution coefficient D (L/g) [$D = q_e$ (mmol/g)/C_e (mmol/L)]. Figure 8 illustrated the affinity of ACPAN fibers with the metals was in the order: $UO_2^{2+} \gg Ba^{2+} > Zn^{2+} > Sr^{2+} > Fe^{3+} > Cr^{3+} > Cu^{2+} > Ca^{2+} > Ni^{2+} > Mg^{2+}$. This also showed that uranium formed a more stable complex with ACPAN fibers.

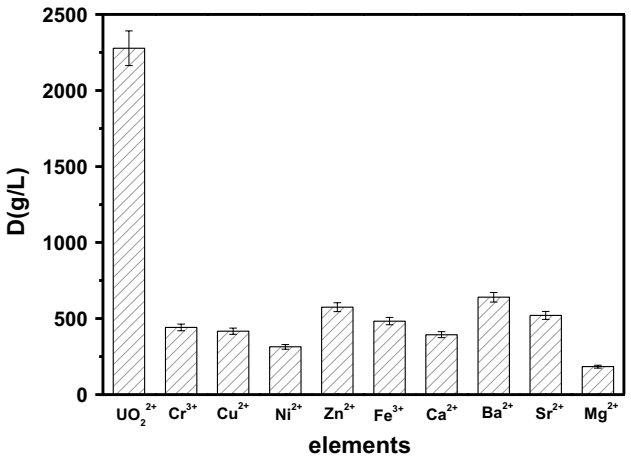

Fig. 8 adsorption of uranium and other metal ions on ACPAN fibers. $I = 0.1$ mol/L, pH = 5.0 ± 0.1, $C_0 = 4\times10^{-4}$ mol/L, $T = 298 \pm 1$ K, $t = 48$ h

The above results suggested that metal ions have certain effect on uranium extraction by ACPAN fibers, but their effect was not as significant as the solution pH, which indicated that ACPAN fibers had a strong affinity with U(VI) ions in aqueous solutions and ACPAN fibers had very high selectivity for the recovery of uranium. The results demonstrated that ACPAN fibers can be used as a promising adsorbent to selectively extract uranium.

Desorption and reusability studies

Desorption experiments were conducted to study the eluting performance of ACPAN fibers and the possibility of regeneration. The desorption of UO_2^{2+} from the ACPAN fibers was studied by using 0.1M citric acid, 1M citric acid, 0.5M Na_2CO_3, 1M Na_2CO_3, 2M Na_2CO_3. The regents were chosen based on the literature related to uranyl elution [3, 33, 40], and the results were shown in Fig. 9. It showed that most of the regents cannot elute uranyl with a considerable amount, except Na_2CO_3. Moreover, with Na_2CO_3 concentration increasing, uranyl eluted increases until the concentration reached 2M.

The reuse of adsorbent is very important in wastewater treatment. Desorption cycles are crucial to illustrate the stability and potential recovery of the adsorbents. Namely, the adsorbents are further used for adsorption of U(VI) ions after desorption. The adsorption/desorption cycles were tested five times in this work and the results were shown in Fig. 10. A slight and progressive decrease of the adsorption capacity was observed. The percentage removal of U(VI)

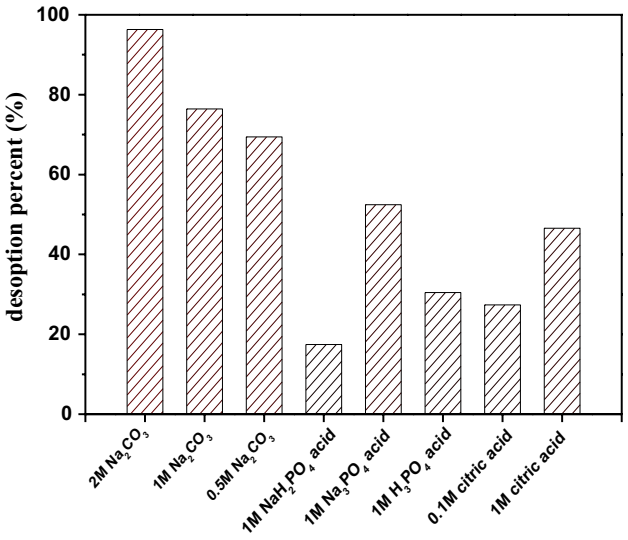

Fig. 9 desorption of U(VI) ions from ACPAN fibers using various types of eluents

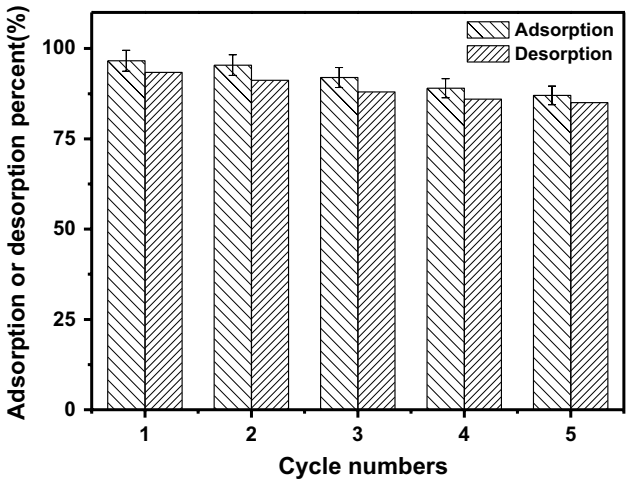

Fig. 10 consecutive sorption/desorption cycles of the ACPAN fibers for 0.1 mmol/L U(VI) solution using 2 M Na_2CO_3 as the desorbing agent, $T = 298 \pm 1$ K, $I = 0.1$ mol/L, $t = 48$ h

ion was 88% for ACPAN fibers at 5rd cycle. Desorption by 2M Na_2CO_3 solution easily occurring might be related to the intensive competition between CO_3^{2-} ions and metal ions on the active sites. These results indicated that the ACPAN fibers have the potential of regeneration and reuse.

Adsorption mechanisms

In order to further speculate the U(VI) adsorption mechanism on ACPAN fibers, FTIR and XPS of samples were studied. Figure 1d displayed FT-IR spectra of uranyl loaded on ACPAN fibers at pH 5. After U(VI) adsorbed, some new peaks appeared at 1038, 948, 826 cm^{-1}, and other peaks have shifted or weakened. The FT-IR peaks of U(VI) adsorbed on ACPAN fibers were markedly red shifted as compared to the FT-IR peak for aqueous U(VI) at ~963 cm^{-1}, and peak at 826 cm^{-1} assigned to U=O symmetry stretching vibration of U(VI) [21, 41, 42]. The characteristic absorption peak of ACPAN fibers at 1590 cm^{-1} (in Fig. 1c) which was due to the

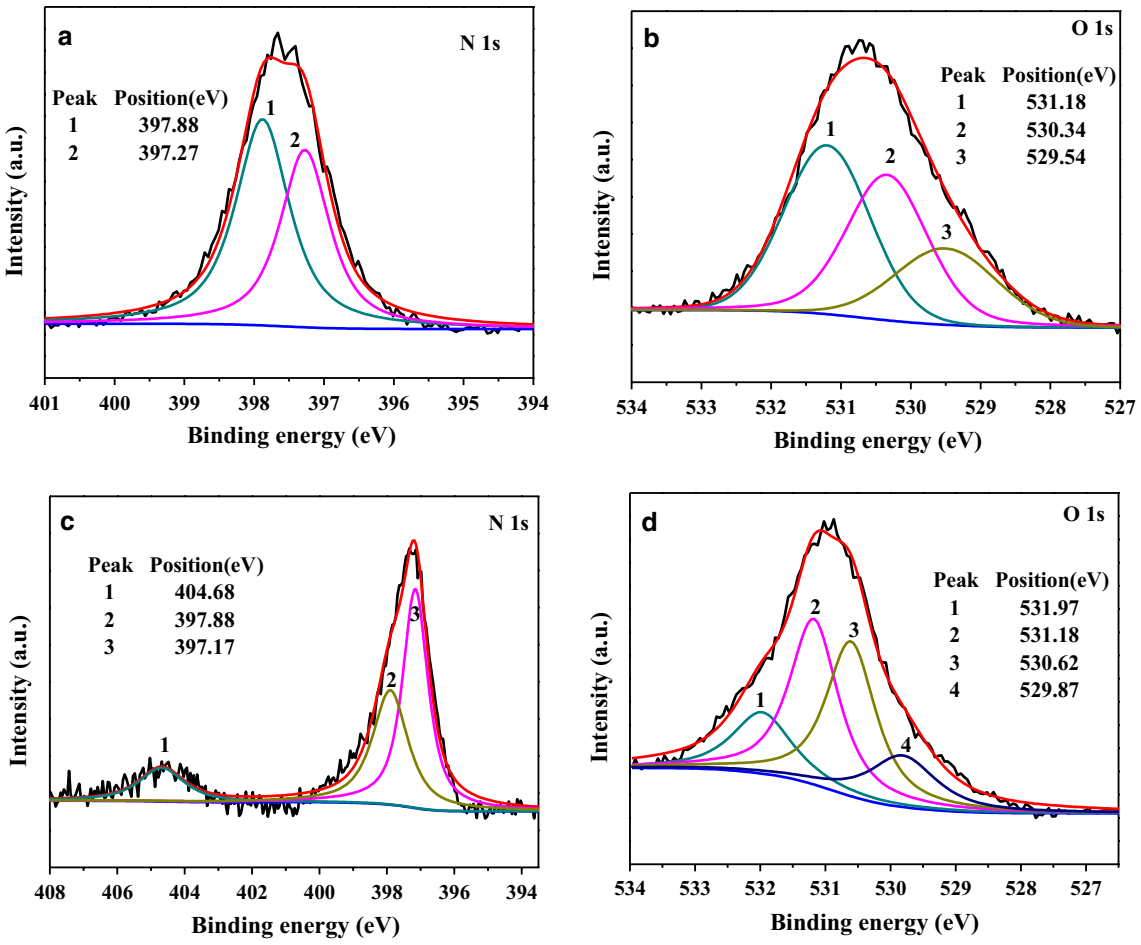

Fig. 11 XPS spectra of ACPAN fibers and uranyl-loaded ACPAN fibers, ACPAN fibers of N1*s* and O1*s* of XPS spectra (**a**, **b**); uranyl-loaded ACPAN fibers of N1*s* and O1*s* of XPS spectra (**c**, **d**)

Table 5 XPS parameters (N1*s* and O1*s*) of ACPAN fibers and loaded U(VI)-ACPAN fibers

N1*s*	$-NH_2$ (eV)	–NO (eV)	New peak (eV)
Before adsorption U(VI)	397.27	397.88	
After adsorption U(VI)	397.17	397.88	404.68
O1*s*	–OH (eV)	–NO (eV)	–CO (eV)	New peak (eV)
Before adsorption U(VI)	531.18	530.34	529.54	
After adsorption U(VI)	531.18	530.62	529.87	531.97

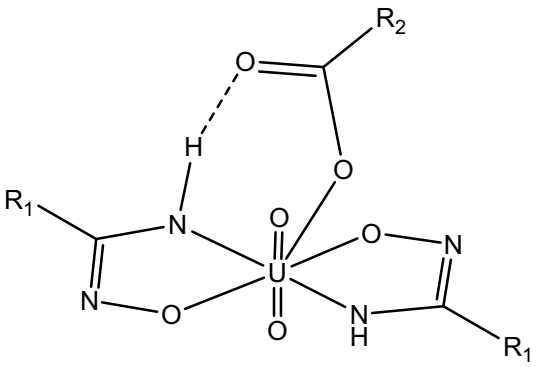

Scheme 1 Coordination modes of uranium with ACPAN fibers

bending vibration of $-NH_2$, disappeared and meanwhile gave rise to a new strong absorption band (in Fig. 1d) at 1038 cm^{-1}, which can be attributed to the complexed uranyl ions with N–H. Comparing the Fig. 1d to c, the N–O peak of Fig. 1c in 915 cm^{-1} shifted to the low wave number of 902 cm^{-1}, which also indicated that O atom in N–O were also coordinated with U(VI). The stretching vibration peak of –OH shifted to the high wave number and the bending vibration peak shifted to the low wave number, which indicated that UO_2^{2+} coordinated with O atom of –OH. Therefore, U(VI) may not only coordinate with Amidoxime's = N–OH/= N–O– and $-NH_2$/–NH– but also with carboxyl group, as can be seen from N–H, C=N, C–N and –N–O peaks of peaks shift (Fig. 1d) and carboxyl peak of intensity became weaker. The result was consistent with previous reports [14].

This adsorption mechanism was further explained by XPS spectra of U(VI) sorption on the ACPAN (in Fig. 11). From Fig. 11, it can be seen that there were two peaks of N1*s* in non-adsorbed U(VI) fibers, corresponding to $-NH_2$ ($E = 397.27$ eV) and –NOH ($E = 397.88$ eV). After adsorbing U(VI), the N1*s* peak corresponding to $-NH_2$ shifted to 0.10 eV, and a new N1*s* peak ($E = 404.68$ eV) appeared, which can be considered as the result of the complexation of amino N with U(VI). However, the N1*s* peak corresponding to –NOH was not shifted. It was concluded that N in the $-NH_2$ of ACPAN participated in the coordination, while N in the NOH may not. On the non-adsorbed U(VI) fibers, O1*s* has three peaks, corresponding to –OH ($E = 531.18$ eV), N–O ($E = 530.34$ eV) and C–O ($E = 529.54$ eV), respectively. After the adsorption of U(VI), the O1*s* peak corresponding to N–O shifted 0.32 eV, and corresponding to the C-O also shifted 0.33 eV, meanwhile a new O1*s* peak ($E = 531.97$ eV) appeared. It can be concluded that O on amidoxime group and the carboxyl oxygen atom of ACPAN fibers were involved in the complexation of U(VI). XPS parameters (N1*s* and O1*s*) of ACPAN fibers and loaded U(VI)-ACPAN fibers were shown in Table 5. Probable complexation model of uranium with ACPAN fibers showed in Scheme 1. The result was in line with that of Wang et al. by FTIR and DFT calculation [14].

Conclusion

This work showed that ACPAN fibers have a high adsorption capacity for U(VI) and can be effectively used for the rapid removal of uranyl ions from aqueous solutions. The adsorption of uranyl depended on the U(VI) concentration, contact time, pH and temperature. The adsorption of uranyl on ACPAN fibers was well described by pseudo-second-order model and the adsorption equilibrium conformed to Freundlich isotherm and D–R model. Adsorption of uranyl ions on ACPAN fibers occurred as a spontaneous and endothermic process. The adsorption/desorption experimental results displayed that ACPAN fibers had exceptional reusability. The maximum adsorption capacity was 163 mg/g. In summary, ACPAN fibers is an effective adsorbent for removal of uranium(VI) from industrial wastewater.

Acknowledgements The authors thank to the financial support of the National Natural Science Foundation of China (Nos. 21641003 and 21976074).

Compliance with ethical standards

Conflict of interest The authors declare that they have no competing interests.

References

1. Kharecha PA, Hansen JE (2013) Prevented mortality and greenhouse gas emissions from historical and projected nuclear power. Environ Sci Technol 47:4889–4895
2. Camacho LM, Deng SG, Parra RR (2010) Uranium removal from groundwater by natural clinoptilolite zeolite: effects of ph and initial feed concentration. J Hazard Mater 175:393–398
3. Barber PS, Kelley SP, Rogers RD (2012) Highly selective extraction of the uranyl ion with hydrophobic amidoxime functionalized ionic liquids via η^2 coordination. RSC Adv 2:8526–8530
4. Pan DQ, Fan QH, Ding KF, Li P, Lu Y, Yu T, Xu J, Wu WS (2011) The sorption mechanisms of Th(IV) on attapulgite. Sci China Chem 54(7):1138–1147
5. Zeinab FA, Shymaa ME, Ayman MA (2016) In-situ synthesis of magnetite acrylamide amino- amidoxime nanocomposite adsorbent for highly efficient sorption of U(VI) ions. J Ind Eng Chem 34:105–116
6. Yu SJ, Wang XX, Yang ST, Sheng GD, Alsaedi A, Hayat T, Wang XK (2017) Interaction of radionuclides with natural and manmade materials using XAFS technique. Sci China Chem 60(2):170–187
7. Kim J, Tsouris C, Mayes RT, Tsouris C, Mayes RT, Oyola Y, Saito T, Janke CJ, Dai S, Schneider E, Sachde D (2013) Recovery of uranium from seawater: are view of current status and future research needs. Sep Sci Technol 48:367–387
8. Rao L (2011) Recent international R&D activities in the extraction of uranium from seawater. Lawrence Berkeley National Laboratory, Berkeley
9. Seko N, Tamada M, Yoshii F (2005) Current status of adsorbent for metal ions with radiation grafting and crosslinking techniques. Nucl Instrum Methods Phys Res Sect B 236:21–29
10. Zhao HH, Liu XY, Yu M, Wang ZQ, Zhang BW, Ma HJ, Wang M, Li JY (2015) A study on the degree of amidoximation of polyacrylonitrile fibers and its effect on their capacity to adsorb uranyl ions. Ind Eng Chem Res 54(12):3101–3106
11. Zhang XF, Yang SY, Yu B, Tan QL, Zhang XY, Cong HL (2018) Advanced modified polyacrylonitrile membrane with enhanced adsorption property for heavy metal ions. Sci Rep 8:1260
12. Choi YH, Choi CM, Choi DH, Paik YK, Park BJ, Joo YK, Kim NJ (2011) Time dependent solid-state ^{13}C NMR study on alkaline hydrolysis of polyacrylonitrile hollow fiber ultrafiltration membranes. J Membr Sci 371(1–2):84–89
13. Chen ZJ, Huang NH, Liu H (2013) The hydrophilic properties of polyacrylonitrile fiber modified with acrylamide. J Wuhan Text Univ 26(6):32–36
14. Xiong J, Hu S, Liu Y, Yu J, Yu HZ, Xie L, Wen J, Wang XL (2017) Polypropylene modified with amidoxime/carboxyl groups in separating uranium(VI) from thorium(IV) in aqueous solutions. ACS Sustain Chem Eng 5(2):1924–1930
15. Liu XY, Liu HZ, Ma HJ, Cao CQ, Yu M, Wang ZQ, Deng B, Wang M, Li JY (2012) Adsorption of the uranyl ions on an amidoxime-based polyethylene nonwoven fabric prepared by preirradiation-induced emulsion graft polymerization. Ind Eng Chem Res 51:15089–15095
16. Gupta ML, Gupta B, Oppermann W, Hardtmann G (2004) Surface modification of poly- acrylonitrile polyacrylonitrile staple fibers via alkaline hydrolysis for superabsorbent applications. J Appl Polym Sci 91:3127–3133
17. Jia Z, Yang YG (2007) Surface modification of polyacrylonitrile (PAN) fibers by grafting of natural polymer-soy protein. Polym Bull 59:13–23
18. Choi SH, Nho YC (2000) Adsorption of UO_2^{+2} by polyethylene adsorbents with amidoxime, carboxyl, and amidoxime/carboxyl group. Radiat Phys Chem 57:187–193
19. Das S, Brown S, Mayes RT, Janke CJ, Tsouris C, Kuo LJ, Gill G, Dai S (2016) Novel poly(imide dioxime) sorbents: development and testing for enhanced extraction of uranium from natural seawater. Chem Eng J 298:125–135
20. Han ZB, Guo J, Li W (2013) $Fe(bpy)_3^{2+}$supported on amidoximated PAN fiber as effective catalyst for the photo degradation of organic dye under visible light irradiation. Chem Eng J 228:36–44
21. Zhao YG, Shen HY, Pan SD, Hu MQ, Xia QH (2010) Preparation and characterization of amino-functionalized nano-Fe_3O_4 magnetic polymer adsorbents for removal of chromium (VI) ions. J Mater Sci 45:5291–5301
22. Özcan A, Öncü E, Özcan AS (2006) Kinetics, isotherm and thermodynamic studies of adsorption of acid blue 193 from aqueous solutions onto natural sepiolite. Colloids Surf A 277:90–97
23. Kago T, Goto A, Kusakabe K, Morooka S (1992) Preparation and performance of amidoxime fiber adsorbents for recovery of uranium from seawater. Ind Eng Chem Res 31(1):204–209
24. Wu FC, Tseng RL, Juang RS (2009) Initial behavior of intraparticle diffusion model used in the description of adsorption kinetics. Chem Eng J 153(1):1–8
25. Egawa H, Kabay N, Jyo A, Hirono M, Shuto T (1994) Recovery of uranium from seawater. 15. Development of amidoxime resins with high sedimentation velocity for passively driver fluidized bed adsorbers. Ind Eng Chem Res 33:657–661
26. Wang CZ, Lan JH, Wu QY, Luo Q, Zhao YL, Wang XK, Chai ZF, Shi WQ (2014) Theoretical insights on the interaction of uranium with amidoxime and carboxyl groups. Inorg Chem 53:9466–9476
27. Niu ZW, Fan QH, Wang WH, Xu JZ, Chen L, Wu WS (2009) Effect of pH, ionic strength and humic acid on the sorption of uranium(VI) to attapulgite. Appl Radiat Isot 67:1582–1590
28. Pekel N, Güven O (2003) Separation of uranyl ions with amidoximated poly(acrylonitrile/N-vinylimidazole) complexing sorbents. Colloids Surf A Physicochem Eng Asp 212:155–161
29. Wang GH, Liu JS, Wang XG, Xie ZY, Deng NS (2009) Adsorption of uranium (VI) from aqueous solution onto cross-linked chitosan. J Hazard Mater 168:1053–1058
30. Ji LL, Chen W, Bi J, Zheng SR, Xu ZY, Zhu DQ, Alvarez PJ (2010) Adsorption of tetracycline on single-walled and multiwalled carbon nanotubes as affected by aqueous solution chemistry. Environ Toxicol Chem 29:2713–2719
31. Alberghina G, Bianchini R, Fichera M, Fisichella S (2000) Dimerization of Cibacron Blue F3GA and other dyes: influence of salts and temperature. Dyes Pigm 46:129–137
32. Wu ZJ, Liu HN, Zhang HF (2010) Research progress on mechanisms about the effect of ionic strength on adsorption. Environ Chem 29(6):997–1003
33. Li WP, Han XY, Wang XY, Wang YQ, Wang WX, Hu H, Tan TS, Wu WS, Zhang HX (2015) Recovery of uranyl from aqueous solutions using amidoximated polyacrylonitrile/exfoliated Na-montmorillonite composite. Chem Eng J 279:735–746
34. Zhao DL, Zhu HY, Wu CN, Feng SJ, Alsaedi A, Hayat T, Chen CL (2018) Facile synthesis of magnetic Fe_3O_4/graphene composites for enhanced U(VI) sorption. Appl Surf Sci 444:691–698
35. Ma Y, Zhou Q, Zhou SC, Wang W, Jia JJ, Xie W, Li AM, Shuang CD (2014) A bifunctional adsorbent with high surface area and cation exchange property for synergistic removal of tetracycline and Cu^{2+}. Chem Eng J 258:26–33
36. Glasstone S, Laidler KJ, Eryring H (1941) The theory of rate processes. McGraw-Hill, New York
37. Bai J, Yin XJ, Zhu YF, Fan Fl WuXL, Tian W, Tan CM, Zhang X, Wang Y, Cao SW, Fan FY, Qin Z, Guo JS (2016) Selective uranium sorption from salt lake brines by amidoximated Saccharomyces cerevisiae. Chem Eng J 283:889–895
38. Manos MJ, Kanatzidis MG (2012) Layered metal sulfides capture uranium from seawater. J Am Chem Soc 134:16441–16446

39. Deng S, Bai R, Chen JP (2003) Behaviors and mechanisms of copper adsorption on hydrolyzed polyacrylonitrile fibers. J Colloid Interface Sci 260(2):265–272
40. Zhang A, Uchiyama G, Asakura T (2003) Dynamic-state adsorption and elution behaviour of uranium(VI) ions from seawater by a fibrous and porous adsorbent containing amidoxime chelating functional groups. Adsorpt Sci Technol 21:761–773
41. Shao DD, Jiang ZQ, Wang XK, Li JX, Meng YD (2009) Plasma induced grafting carboxymethyl cellulose on multiwalled carbon nanotubes for the removal of UO_2^{2+} from aqueous solution. J Phys Chem B 113(4):860–864
42. Yang L, Bi L, Lei ZW, Miao Y, Li BL, Liu TH, Wu WS (2018) Preparation of amidoxime functionalized-β-cyclodextrin-graft-(maleic anhydride-co-acrylonitrule) copolymer and evaluation of the adsorption and regeneration properties of Uranium. Polymers 10:236–254